# Automating Treatment Planning in Radiation Therapy

Lekan Ogunmolu

Perelman School of Medicine

University of Pennsylvania, Philadelphia, PA

February 04, 2021

# Funding Sources



NIH NATIONAL CANCER INSTITUTE

THE STATE OF TEXAS

CANCER PREVENTION & RESEARCH INSTITUTE OF TEXAS

# Talk Outline



- Beam Orientation Optimization (BOO)
  - Monte Carlo Tree Search and Neuro-Dynamic Programming for BOO
  - Column Generation as Pretraining for MCTS for BOO
- Patient Head Motion Correction in External Beam Radiation Therapy
  - Intensity-Modulated RT (IMRT): Earlier PhD Work
  - Magnetic Resonance Imaging and Linear Accelerator Systems (MRI-LINACs)
- Robustness Margins and Robust Deep Policies for Nonlinear Control

# Research Significance



2020 → 1.8 million U.S. cancer cases [1] → > 600,000 deaths → 4.2% overall healthcare spending

**Cancer Treatment**
- Chemotherapy/Radiosurgery.
- Radiation Therapy (RT).

**RT Signif.**
- Approx. 40% of all curative cancer treatment modality are performed with RT [Baskar et al].
- Cost-effective -- accounting for only 5% of the total cost of cancer care [Ringborg et al.].

**Imaging**
- CT images in RT = Low soft tissues contrast ⇒ OARs toxicity during treatment planning.
- MRI of brain, and head and neck (H&N) cancers provides exceptional soft tissues contrast and allows greater delineation of cancerous from non-cancerous tissues.

# IMRT Treatment Planning (Beam Delivery)

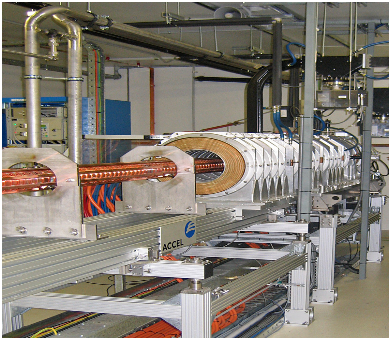


The Australian Synchrotron.

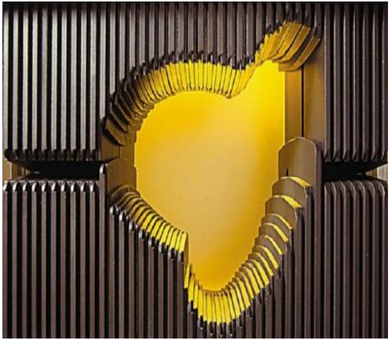

Multi-leaf collimator (Varian)

# Radiation Delivery Couch and Gantry



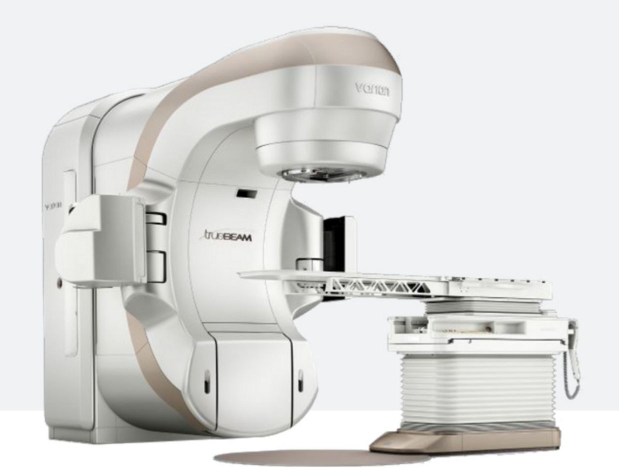


Varian's TrueBeam Radiotherapy System.

# Part I.A: Beam Orientation Optimization (BOO)

- Beam Orientation Optimization (BOO)
  - Monte Carlo Tree Search and Neuro-Dynamic Programming for BOO

# Contributions

## Relevant Publications

Ogunmolu, Olalekan, Michael Folkerts, Dan Nguyen, Nicholas Gans, and Steve Jiang. "Deep BOO! Automating Beam Orientation Optimization in Radiation Therapy." In *Algorithm Foundations of Robotics XIII*, Merida, Mexico. Published in *Springer's Proceedings in Advanced Robotics (SPAR) Book*, 2020.

- A sparse tree lookout strategy for games with large state spaces guides transition between beam angle sets
- Tree lookout strategy guided by a deep neural network policy

# BOO Process: Fluence Map Optimization


Prostate CT slice

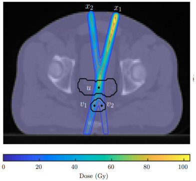


Prostate before BOO

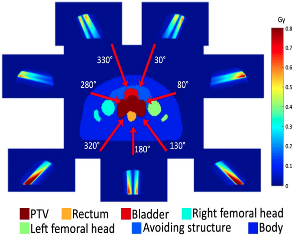


Fluence Map

# Treatment Plan Flowchart

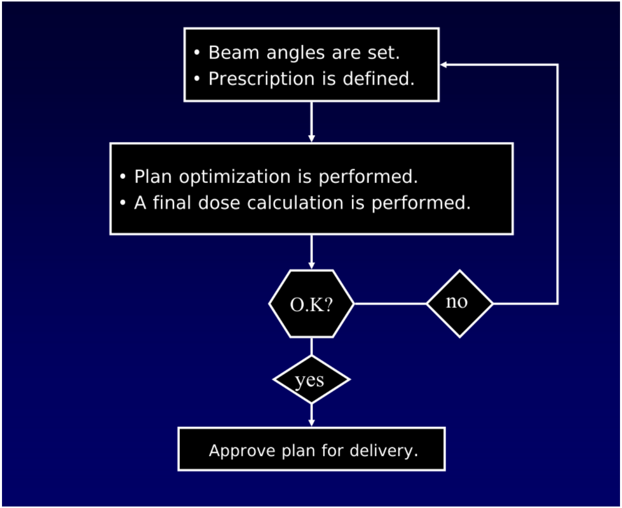


Reprinted from "IMRT Optimization Algorithms. David Shepard. Swedish Cancer Institute. AAPM 2007."

# Current Approaches



- Stochastic optimization approaches: simulated annealing; genetic algorithms and gradient search, or a combination of genetic and gradient search algorithms.
- Mixed-integer programming, branch and cut/bound algorithms, beam angle elimination algorithms.
- Commercial planners use some highly non-convex objective (actual function is proprietary and unknown to public).

# IMRT/BOO Motivation

- Beam orientations largely manually chosen or adopted from a standard protocol for clinical use.
- Pre-solve the dose influence matrices for each beam orientation.
- Then solve FMO.
- Time consuming (hours for dose fluence), and minutes for (FMO); Still solution is often not optimal.

# Approach

- A Tower Neural Network generates a policy that guides MCTS simulations for two players in a zero-sum Markov game
  - Produces a *utility (value) function* & a subjective *probability distribution*
- Each player in a two-player Markov game finds an alternating best response to the current player's average strategy
  - driving the neural network policy's weights toward an approximate **saddle equilibrium** [Heinrich et al. (2015)].
  - aids network in finding an *approximately optimal* beam angle candidate set that meets a dosimetric requirements.

# Data Preprocessing



- 77 anonymized patient CT scans, $\boldsymbol{D}$, and their dose influence matrices, $\mathcal{D}_{ij}$
- Scans shaped, $\boldsymbol{D} \times N \times H \times W$ from prostate cases in previous treatment plans
- Each slice resized to $64 \times 64$

# State Representation: Prostate Organ Masks



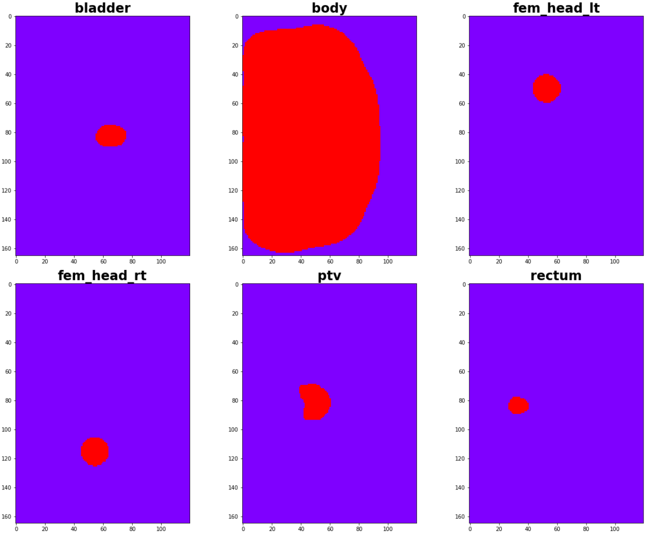

# State Representation: Beam Angles

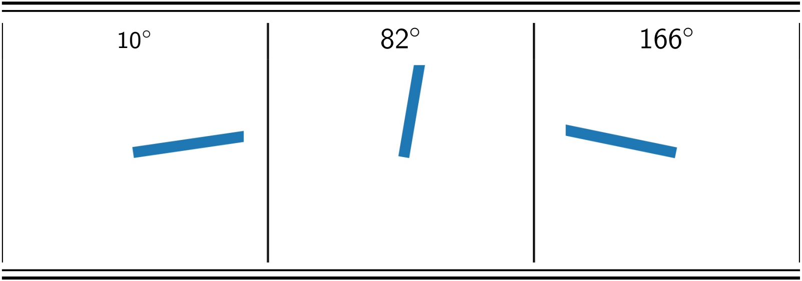

# State Representation

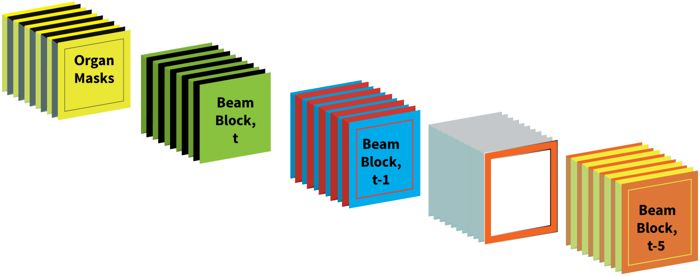

# State Representation

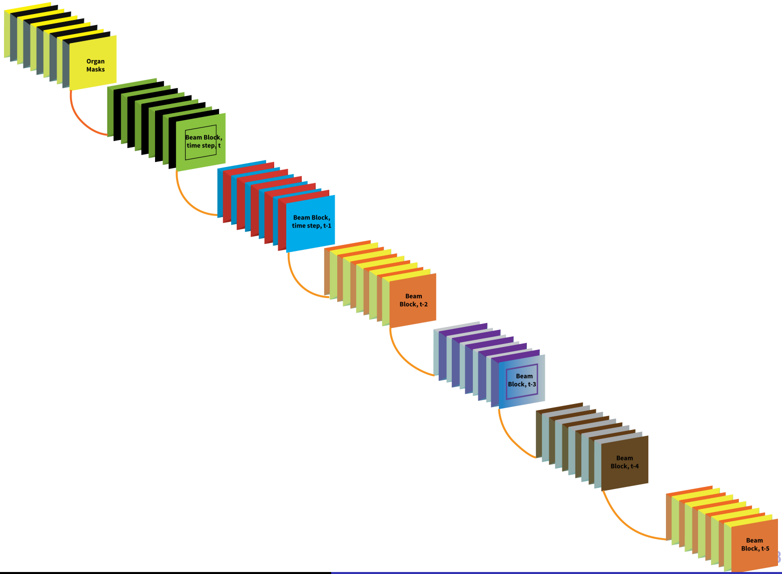

# Tree Representation and Game Simulation



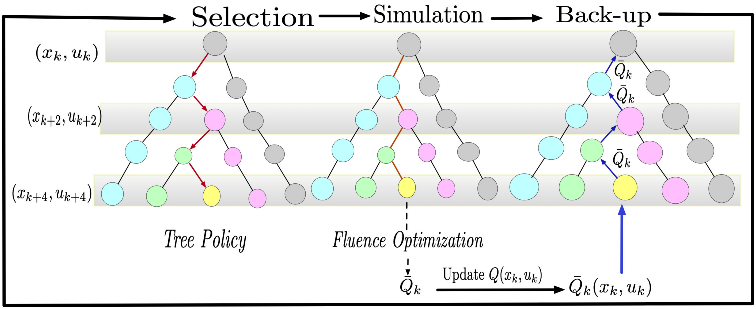

# Tree Composition



Every **node** of the tree, $\boldsymbol{x}$, has the following fields:

- a pointer to the parent that led to it, $\boldsymbol{x}.p$;
- the beamlets, $\boldsymbol{x}_b$, stored at that node; $b = \{1, \ldots, m\}$;
- a set of move probabilities prior, $p(s, a)$;
- a pointer $\boldsymbol{x}.\boldsymbol{r}$, to the reward $r_t$, for the state $\boldsymbol{x}_t$;
- a pointer to the state-action value $Q(s, a)$ and its upper confidence bound $U(s, a)$;
- a visit count $N(s, a)$, that indicates the number of times that node was visited; and
- a pointer $\boldsymbol{x}.child_i$ to each of its children nodes.

# Game Simulation: Mixed Strategies



- Each player, $p_1, p_2$, bases its decision on a random event's outcome
  - generating a **mixed strategy** determined by **averaging the outcome** of individual plays.
- Both players constitute a two-player **stochastic action selection strategy**: $\pi(s, a) = Pr(a|s) := \{\pi^{p_1}, \pi^{p_2}\}$ that gives the probability of selecting moves in any given state
- Suppose the game simulation starts from an initial condition $s_0$.

# Saddle Point Strategy Formulation



- The **saddle point strategies** for an optimal control sequence pair $\{a_t^{p_1^*}, a_t^{p_2^*}\}$ can be recursively obtained by optimizing a state-action value cost, $\mathcal{J}_t(s, a)$

$$V_t^*(s) = Q_t^*(s_t, \pi_t^{p_1}, \pi_t^{p_2}) = \min_{\pi^{p_1} \in \Pi^{p_1}} \max_{\pi^{p_2} \in \Pi^{p_2}} Q_t^\star(s_t, \pi^{p_1}, \pi^{p_2})$$
$$\forall s_t \in \mathcal{S}, \pi^{p_1} \in \Pi^{p_1}, \pi^{p_2} \in \Pi^{p_2}.$$

such that

$$v_{p_1}^\star \leq v^\star \leq v_{p_2}^\star \quad \forall \{\pi_t^{p_1}, \pi_t^{p_2}\}_{0 \leq t \leq T}.$$

where $v_{p_i}^\star$ are the respective optimal values for each player.

# Fluence Map Optimization



- $\mathcal{X} \implies$ total discretized voxels of interest ($VOI$'s) in a target volume
- $\mathcal{B}_1 \cup \mathcal{B}_2 \cup \ldots \cup \mathcal{B}_n \subseteq \mathcal{B} \implies$ beam partition subset
- $\mathcal{D}_{ij}(\theta_k) \implies$ matrix that describes each dose influence, $d_i$
    - Computed by calculating each $d_i$ for every bixel, $j$, at every $\varphi^\circ$, resolution, where $j \in \mathcal{B}_k$

# Methods: FMO problem definition

- Cost

$$\frac{1}{v_s}\sum_{s\in \text{OARs}} \|(b_s - \underline{w}_s \mathcal{D}_{ij}^s \boldsymbol{x}_s)_+\|_2^2 + \frac{1}{v_s}\sum_{s\in \text{PTVs}} \|(\bar{w}_s \mathcal{D}_{ij}^s \boldsymbol{x}_s - b_s)_+\|_2^2 \tag{1}$$

- Pre-calculated dose term: $\boldsymbol{Ax} = \{\sum_s \frac{w_s}{v_s}\mathcal{D}_{ij}^s \boldsymbol{x}_s \,|\, \mathcal{D}_{ij} \in \mathbb{R}^{n\times l}, n > l\}$

# Methods: FMO

- Rewriting the objective

$$\min \frac{1}{2}\|A\mathbf{x} - \mathbf{b}\|_2^2 \quad \text{subject to } x \geq 0.$$

- With Lagrangian:

$$L(\boldsymbol{x}, \boldsymbol{\lambda}) = \min \frac{1}{2}\|A\mathbf{x} - \mathbf{b}\|_2^2 - \boldsymbol{\lambda}^T \boldsymbol{x}.$$

- Introducing an auxiliary variable $\mathbf{z}$, we have

$$\min_{\boldsymbol{x}} \frac{1}{2}\|\boldsymbol{A}\boldsymbol{x} - \mathbf{b}\|_2^2, \quad \text{subject to } \boldsymbol{z} = \boldsymbol{x},\ \boldsymbol{z} \geq 0,$$

# Methods: FMO by way of ADMM



- Solving either the $\boldsymbol{x}$ and $\boldsymbol{z}$ sub-problems, we have

$$\boldsymbol{x}^{k+1} = \left(\boldsymbol{A}^T\boldsymbol{A} + \rho\boldsymbol{I}\right)^{-1}\left(\boldsymbol{A}^T\boldsymbol{b} + \rho\boldsymbol{z}^k - \boldsymbol{\lambda}^k\right). \tag{2}$$

- And using the soft-thresholding operator, $S_{\boldsymbol{\lambda}/\rho}$, we find that

$$\boldsymbol{z}^{k+1} = S_{\boldsymbol{\lambda}/\rho}\left(\boldsymbol{x}^{k+1} + \boldsymbol{\lambda}^k\right), \tag{3}$$

where $S_{\boldsymbol{\lambda}/\rho}(\tau) = (x - \boldsymbol{\lambda}/\rho)_+ - (-\tau - \boldsymbol{\lambda}/\rho)_+$. $\boldsymbol{\lambda}$ is updated as

$$\boldsymbol{\lambda}^{k+1} = \boldsymbol{\lambda}^k - \gamma(\boldsymbol{z}^{k+1} - \boldsymbol{x}^{k+1}), \tag{4}$$

where $\gamma$ is a parameter that controls the step length.

# Training and Validation Loss

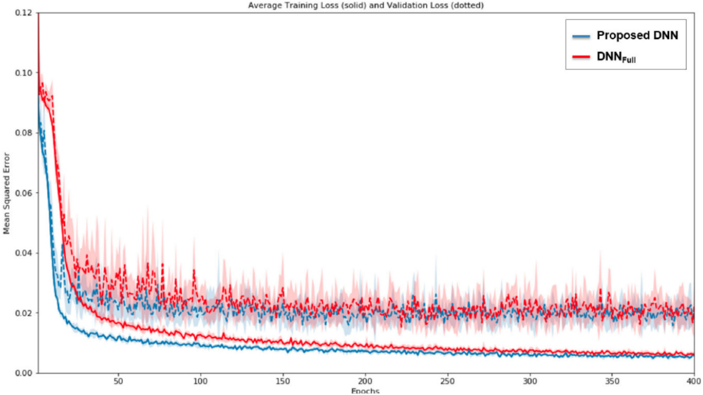


*Average training (solid) and validation (dotted) loss function (MSE) values across six cross-validation folds for the network (blue) and full network.*

# BOO Results: Testing of self-play network

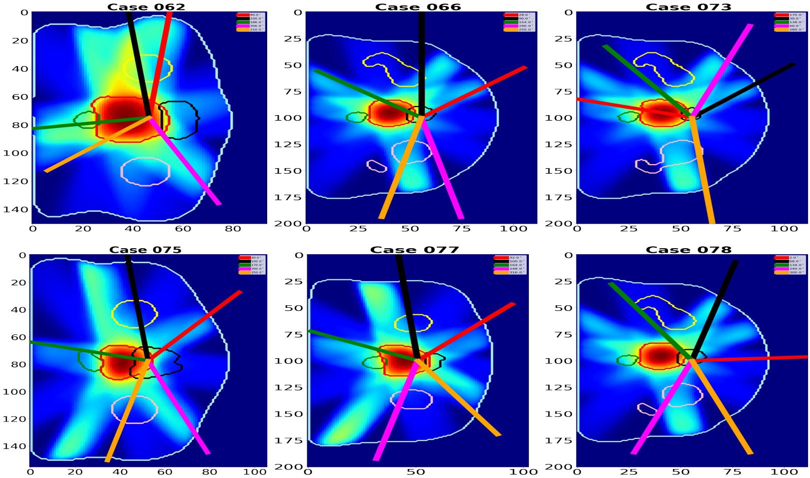

# Dose Washes of Column Generation vs Neural Network

Automating Treatment Planning in Radiation Therapy

Lekan Ogunmolu

BOO
MCTS
BOO Motivation
Approach

Head Stabilization
IMRT
MRI-LINAC

iDG
Robustness issues
Approach
iDG Results

Future Work

Publications

References

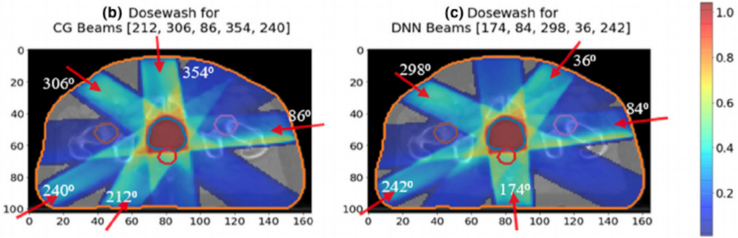


Dose-Volume Histogram of CG vs DNN architectures [Sadeghnejad Barkousaraie, Azar and Ogunmolu, Olalekan and Jiang, Steve and Nguyen, Dan (2019)].

# Dose Volume Histograms

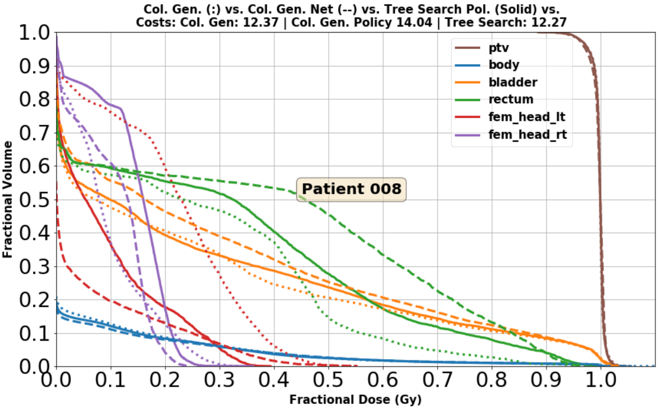

# Conclusions



- Finding the good beam angle candidates is orders of magnitude faster than the current approaches
  - Based on a neural network generative model of an MDP
  - Sparse lookahead search builds tree with nodes labeled by state-action pairs in an alternating manner (2-3 minutes).
  - Tree built stagewise from root to nodes has fixed depth; sample rewards stored on edges connecting state-action with state nodes
- Beam angles prediction takes between 2-3 minutes with MCTS vs 1 minute with Column Generation Pretraining.

# Head Stabilization in Radiation Therapy (RT)

- Head Stabilization in Cancer Radiation Therapy
  - Intensity-Modulated RT (IMRT)

# Varian's TrueBeam Radiotherapy System.



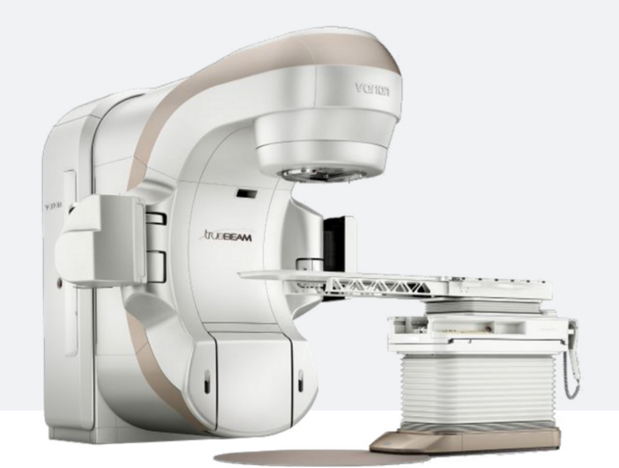

# Correcting Head Motion: RT and MRI-LINACs



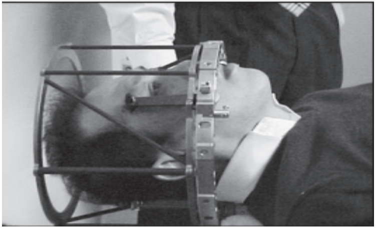

(a) The BRW SRS Frame [Chelvarajah et al. (2004)]


(b) Thermoplastic masks

(c) Frame With MRI Coils (PSOM)

# 4-D Motion Correction Stage

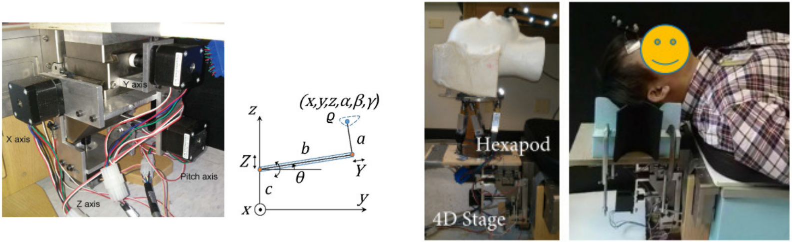


Liu et al. (2015)

# 4-DOF Motion Controller Block Diagram

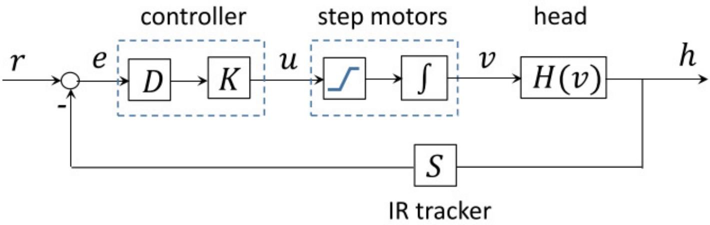


Liu et al. (2015)

# Phantom Feedback Motion Correction Results

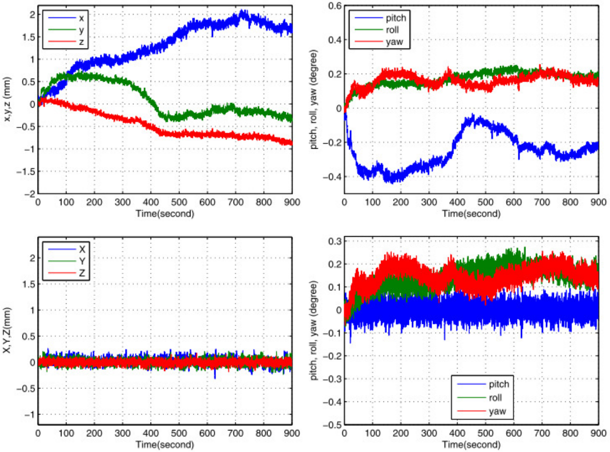


Time response of feedback control without (left) and with (right) decoupling control [Liu et al. (2015)].

# Human Volunteer Feedback Motion Correction Results

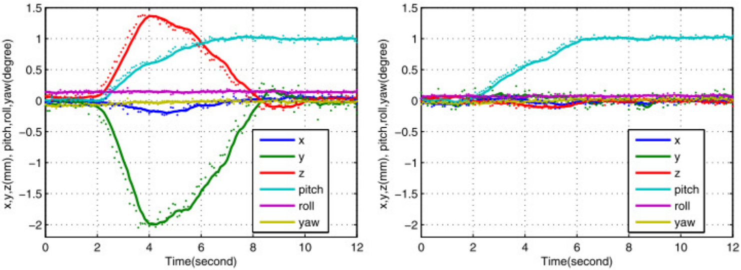


Head Motion Without and With Motion Correction. Left: Coupled Axes; Right: Decoupled Axes.

# SRS: Wiersma Stewart-Gough Platform



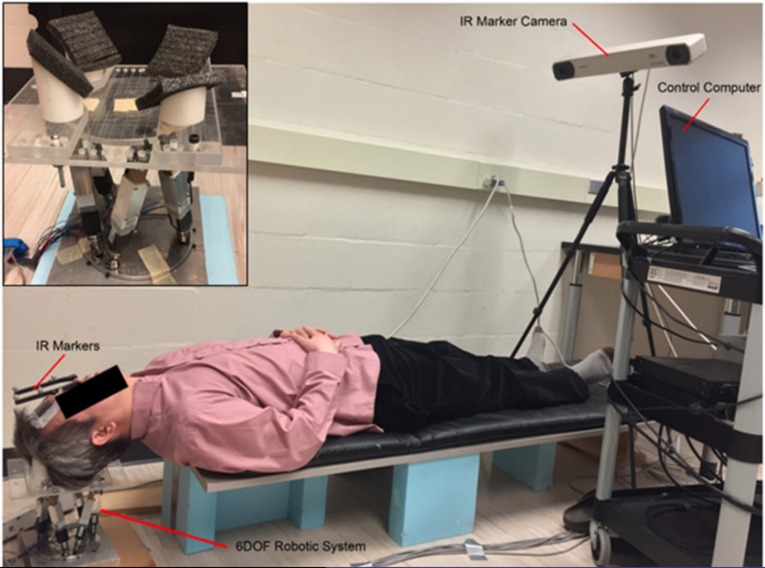

# 6-DOF Motion Correction Results



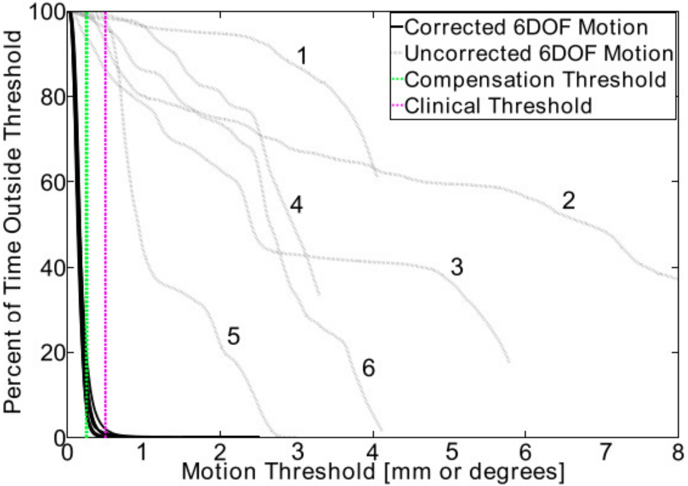

# Drawbacks of current solutions



- Rigid patient's body assumption
- Non-compliant immobilization devices
- Invasiveness during radiosurgery/RT
- Attenuation of photon beams

# Robotic Radiosurgery



Penn
UNIVERSITY *of* PENNSYLVANIA

## A Patient Head Motion-Correction Mechanism for MRI-LINAC RT

OLALEKAN OGUNMOLU
DEPARTMENT OF RADIATION ONCOLOGY, PENN SCHOOL OF MEDICINE

- Current Collaborators: Rodney Wiersma & Xinmin Liu (UChicago → UPenn)
- Past Collaborators: Steve Jiang, Xuejun Gu, (UT Southwestern); Nick Gans (UT Dallas, UT Arlington)

# Radiation Delivery Couch and Gantry



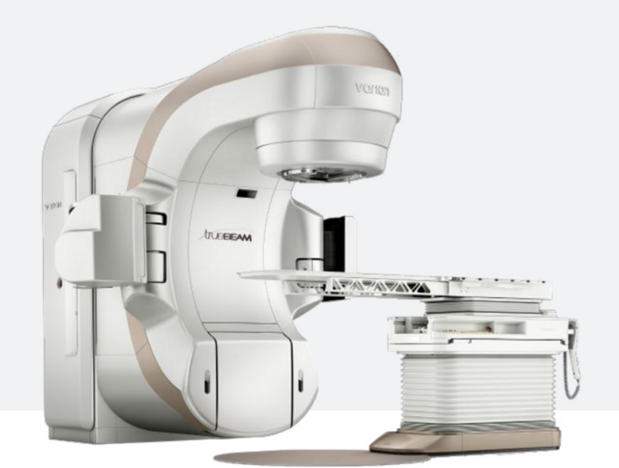


Varian's TrueBeam Radiotherapy System.

# Next-Gen RT Treatment with MRI-LINACs


Elekta's Unity MRI-LINAC. Elekta

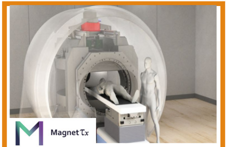


**MRI**DIAN by ViewRay: MR image guidance Radiation on table Adaptive Radiotherapy.

VIEWRAY®

## MRI in LINAC RT

- Next generation precision beam delivery.
- High speed, high resolution MLC.
- Online plan adaptation capabilities.

---

- MRI that offers superior soft tissues visualization integrated with linear accelerator (LINAC) RT Offers unrivaled, online, and real-time cancer RT treatment [Raaymakers et al., Raaymakers et al.]
- Commercialized in systems such as
  - Elekta AB's (Sweden) 1.5T diagnostic imaging system [Raaymakers et al.];
  - Viewray 's MRIdian system [Mutic et al.]; or
  - the MagnetTx's (Canada) Aurora RT system [Fallone et al.] among others.
- Random and involuntary patient motion often occurs during image acquisition leading to
  - Artifacts ⇒ Poor image quality.
  - Incomplete irradiation of the tumor target.
  - Exposure of healthy tissues to radiation toxicity.
    - These lower the accuracy of online and real-time precise radiation dose delivery.
    - Affects clinical efficacy.

# Pneumatic Actuated Soft Robots for Head Motion Compensation



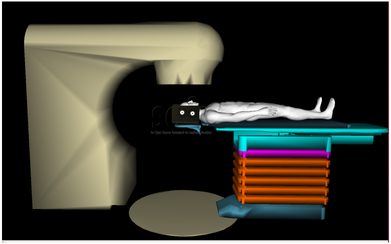

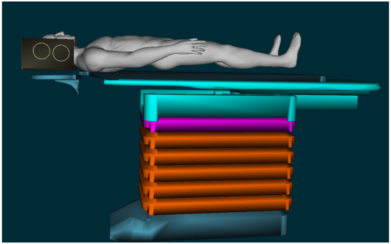

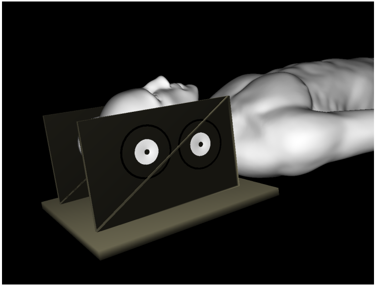

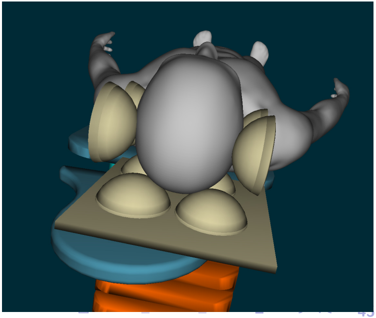

# Cephalopods-inspired CCOARSE Actuator Design



Circumferentially Constrained And Radially Symmetric Elastomers [Pikul et al. (2019)].

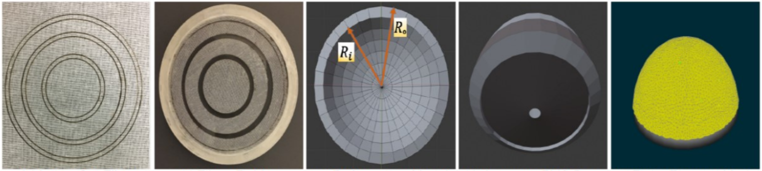


(a) Laser-Cut Fiber (b) Fiber+Rubber (c) Deformation Model (d) Actuator+PVC Base (e) Finite Element Model

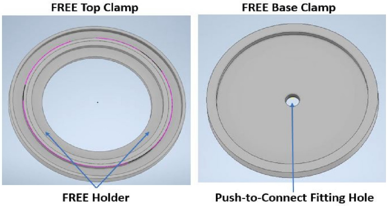


(f,g)

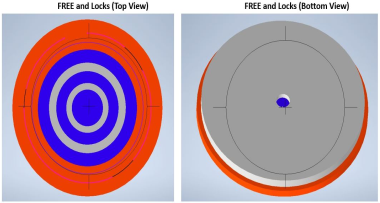


(h)

# CCOARSE Actuator Schematic

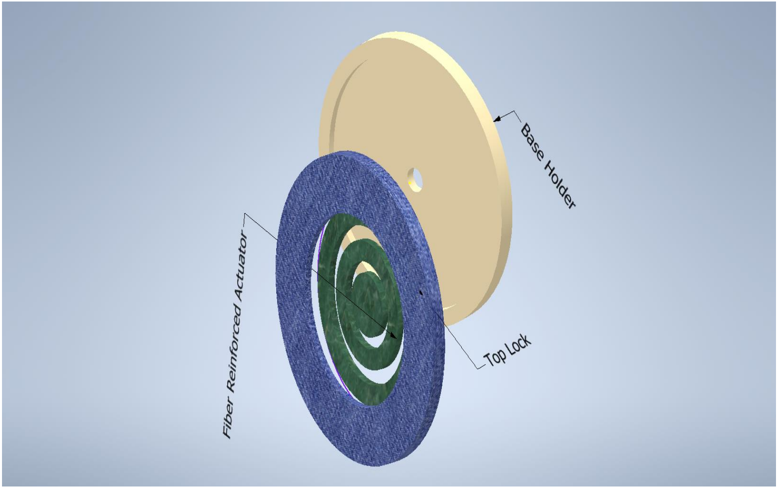

# Nonlinear Elastic Deformation Analysis

IAB SHELLS AND AIR CAVITY/DEFORMATION ANALYSIS

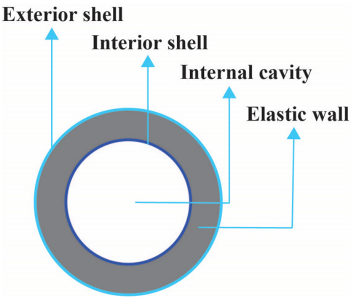


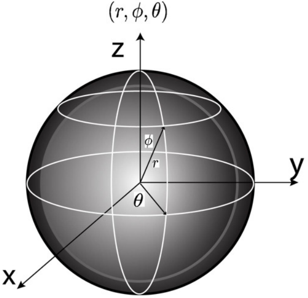


$r_i \leq r \leq r_o, \qquad 0 \leq \theta \leq 2\pi, \qquad 0 \leq \phi \leq \pi$

# Soft IK via Boundary Value Problem

- Using the following boundary conditions for the Cauchy Stress,
  - $\sigma_{rr|R=R_0} = -P_{atm}, \sigma_{rr|R=R_i} = -P_{atm} - P$
- And together with Cauchy's first law, we find that
  - $\sigma_{rr}(r) = -\int_{r_i}^{r_o}[2C_1(\frac{r}{R^2} - \frac{R^4}{r^5}) + 2\, C_2\left(\frac{r^3}{R^4} - \frac{R^2}{r^3}\right)]dr$
  - $\sigma_{rr}(r) = \int_{R_i}^{R_o}[2C_1\left(\frac{1}{r} - \frac{R^6}{r^7}\right) - 2C_2\left(\frac{R^4}{r^5} - \frac{r}{R^2}\right)]\, dr$
- With $\sigma_{rr|R=R_i} = -P_{atm} - P$ and setting $P_{atm} = 0$, we find
  - $P(r) = \int_{r_i}^{r_o}[2C_1(\frac{r}{R^2} - \frac{R^4}{r^5}) + 2\, C_2\left(\frac{r^3}{R^4} - \frac{R^2}{r^3}\right)]dr$
  - $P(r) = \int_{R_i}^{R_o}[2C_1\left(\frac{1}{r} - \frac{R^6}{r^7}\right) - 2C_2\left(\frac{R^4}{r^5} - \frac{r}{R^2}\right)]\, dr$
  - $r^3 = R^3 + r_i^3 - R_i^3$ and $r_o^3 = R_0^3 + r_i^3 - R_i^3$

# Volumetric Deformation Results (Simulation)



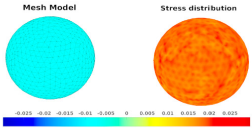


*(a)* **Left**: Mesh model. **Right**: Stress distribution on outer skin.

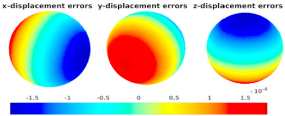


*(b)* Displacement errors along $x, y, z$ coordinates.

| Inputs | | | | | Outputs | | |
|---|---|---|---|---|---|---|---|
| $C_1$ | $C_2$ | $R_i$ | $r_i$ | $R_o$ | $r_o$ | $P$ | $\Delta V$ |
| $1.1e4$ | $2.2e4$ | $.027$ | $.03$ | $.03$ | $.033$ | $.76$ | $\approx 0$ |

Fig. 6: Volumetric Deformation (Expansion).

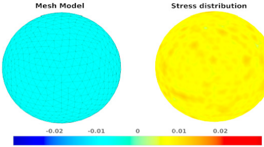


*(a)* **Left**: Mesh model. **Right**: Stress distribution on outer skin.

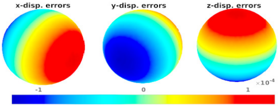


*(b)* Displacement errors along $x, y, z$ coordinates.

| Inputs | | | | | Outputs | | |
|---|---|---|---|---|---|---|---|
| $C_1$ | $C_2$ | $R_i$ | $r_i$ | $R_o$ | $r_o$ | $P$ | $\Delta V$ |
| $1.1e4$ | $2.2e4$ | $.025$ | $.03$ | $.03$ | $.028$ | $-.34$ | $\approx 0$ |

Fig. 7: Volumetric Deformation (Compression).

# Pneumatic Control and Deformation Scheme



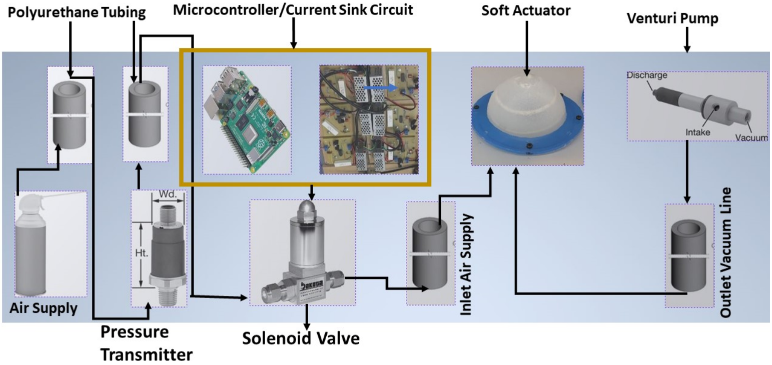

# Volumetric Deformation Results (Actual)



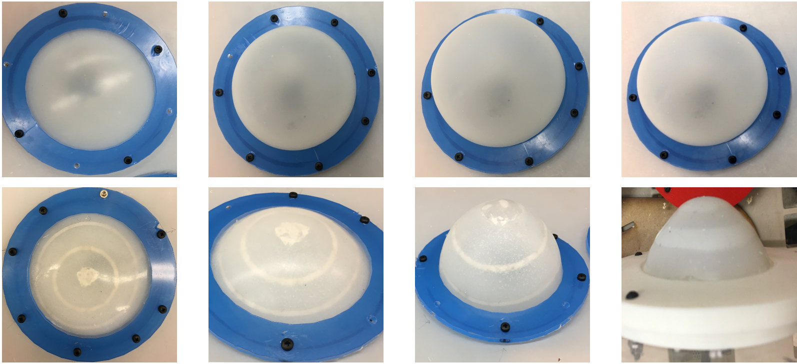

# Mechanism Setup

# Mechanism Setup with Phantom

# Head Motion Control (Independent Actuation)



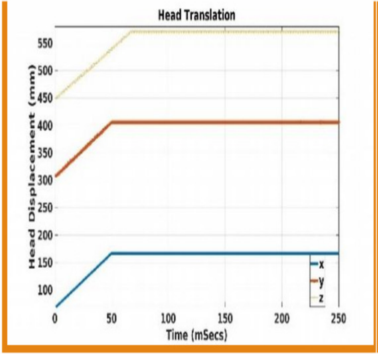


Head Translation along $x, y, z$ for a task of raising the head by a certain threshold above the table

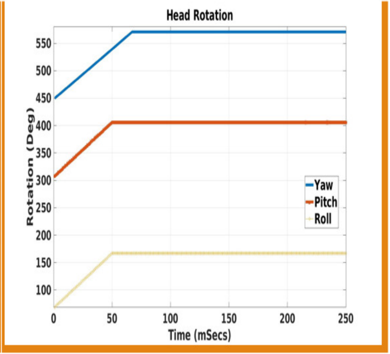


Head rotation in Euler angles for a task of tilting the head about the $x, y, z$ axes on the treatment table.

# Ongoing Work: 6-DOF Closed-loop Control

Continuum Mechanical Model Validation/Differential Geometry/Newton-Euler Dynamics

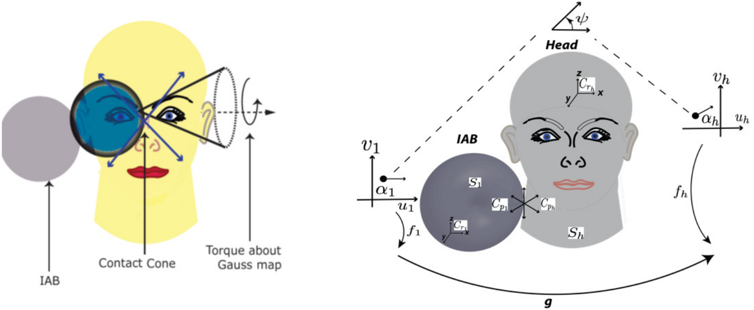

# Pneumatic Actuated Soft Robots for Head Motion Compensation



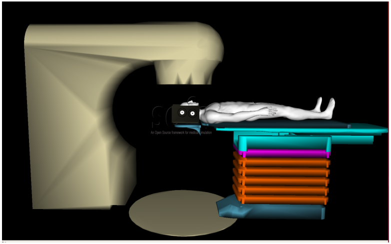

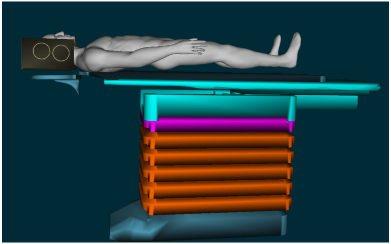

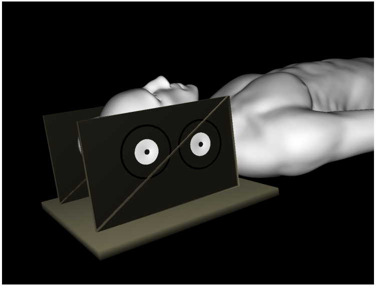

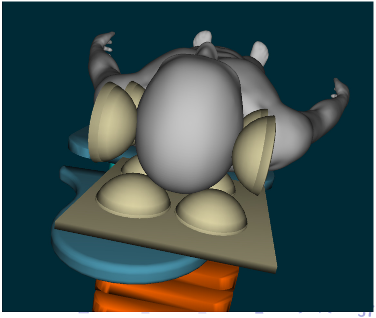

# 3-DOF Simulation Testbed



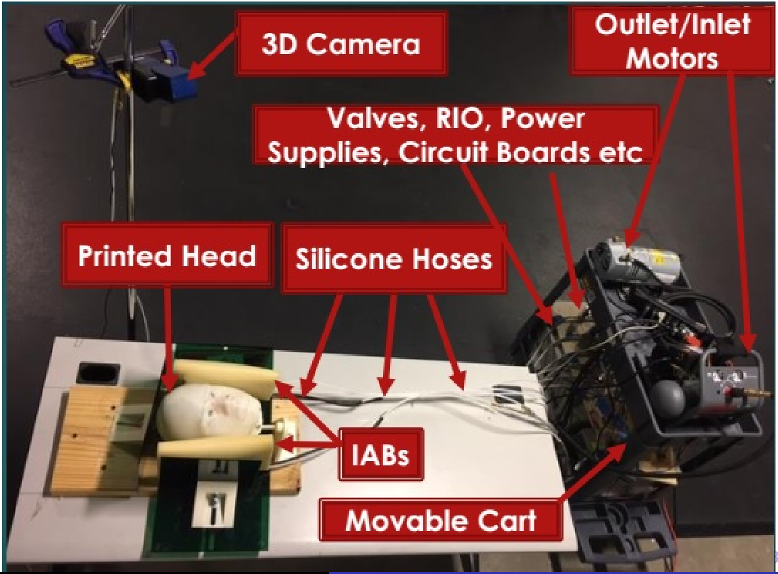

# Control Design Goals



- Stabilize $z$, pitch, and roll states, *i.e.*

$$\boldsymbol{x} = \begin{pmatrix} z \\ \theta \\ \phi \end{pmatrix}$$

- By solving an adaptive state feedback controller, optimal regulation, and minimize parametric uncertainties

# Control Design Goals

- Provide closed loop tracking given a desired trajectory, **r**
- Robustify system to (non-)parametric uncertainties

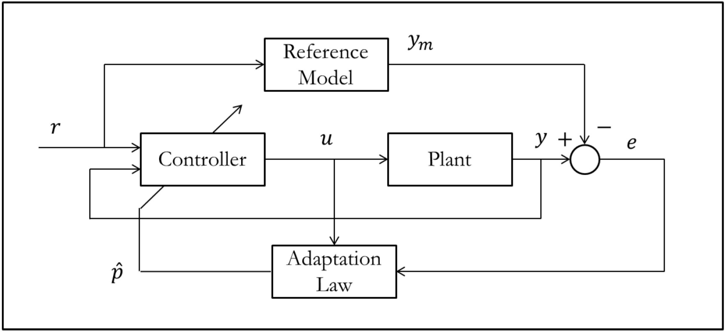


Indirect MRAC system. (Source mdpi.com)

# Model Reference Adaptive Control



- Model head and bladder dynamics as
  - $\dot{\boldsymbol{x}} = \mathbf{A}\boldsymbol{x} + \mathbf{B}\boldsymbol{\Lambda}\left(\mathbf{u} - f(\boldsymbol{x}, \mathbf{u})\right) + \mathbf{w}(k)$
- Approximate $f(\boldsymbol{x}, \mathbf{u})$ by a neural network with continuous memory states
- Derive adaptive adjustment mechanism from Lyapunov analysis for Adaptive Control Parks (1966)
- $\mathbf{u} = \underbrace{\hat{\mathbf{K}}_x^{\mathbf{T}}\boldsymbol{x}}_{\text{state feedback}} + \underbrace{\hat{\mathbf{K}}_r^{\mathbf{T}}\mathbf{r}}_{\text{optimal regulator}} + \underbrace{\hat{f}(\boldsymbol{x}, \mathbf{u})}_{\text{approximator}}$

# Neural Network Architecture

## Neural Net Architecture

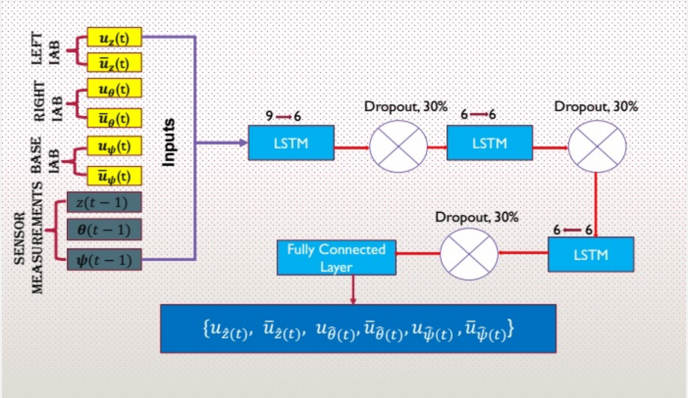

# Lyapunov Redesign: Theorem

- For correct adaptive gains, $\hat{\mathbf{K}}_x$ and $\hat{\mathbf{K}}_r$, $\mathbf{e}(k)$ is ***uniformly ultimately bounded***, and the state $\boldsymbol{x}$ converges to a neighborhood of $\mathbf{r}$.
- Choose a $\mathbf{V}$ in terms of $\mathbf{e}$; $\tilde{\mathbf{K}}_x^T$, $\tilde{\mathbf{K}}_r^T$; and parameter error $\varepsilon_f(\boldsymbol{x}(k))$ space

$$\mathbf{V}(\mathbf{e}, \tilde{\mathbf{K}}_x, \tilde{\mathbf{K}}_r^T) = \mathbf{e}^T\mathbf{P}\mathbf{e} + \mathbf{tr}(\tilde{\mathbf{K}}_x^T \boldsymbol{\Gamma}_x^{-1} \tilde{\mathbf{K}}_x^T |\boldsymbol{\Lambda}|) + \mathbf{tr}(\tilde{\mathbf{K}}_r^T \Gamma_r^{-1} \tilde{\mathbf{K}}_r |\boldsymbol{\Lambda}|)$$

# Stability Results: Ogunmolu et al. (2017)



$$
\begin{aligned}
\dot{\mathbf{V}}(\cdot) &= -\mathbf{e}^T\mathbf{Q}\mathbf{e} - 2\mathbf{e}^T\mathbf{P}\mathbf{B}\boldsymbol{\Lambda}\varepsilon_f \\
&\le -\lambda_{low}\|\mathbf{e}\|^2 + 2\|\mathbf{e}\|\|\mathbf{P}\mathbf{B}\|\lambda_{high}(\boldsymbol{\Lambda})\varepsilon_{max}
\end{aligned}
$$

- $\{\lambda_{low}, \lambda_{high}\} \equiv$ min/max eigenvalues of $Q$ and $\boldsymbol{\Lambda}$.
- $\dot{\mathbf{V}}(\cdot)$ is thus negative definite outside the compact set: $\chi = \left(\mathbf{e} : \|\mathbf{e}\| \le \frac{2\|\mathbf{P}\mathbf{B}\|\lambda_{high}(\boldsymbol{\Lambda})\varepsilon_{max}(\mathbf{y})}{\lambda_{low}(\mathbf{Q})}\right)$
  - *i.e.* $\mathbf{e}$ is **uniformly ultimately bounded**, or $\mathbf{y}(t) \to 0$ as $t \to \infty$.

# Results: Z and Pitch Motions



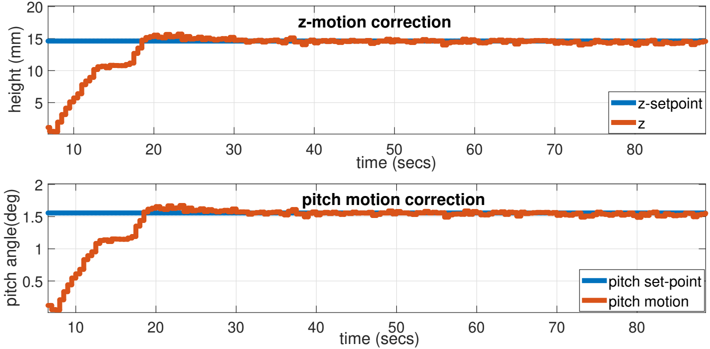


Goal command: $(z, \theta, \phi) = (14mm, 1.6^\circ, 45^\circ)^T$.

# Results: Roll Motion

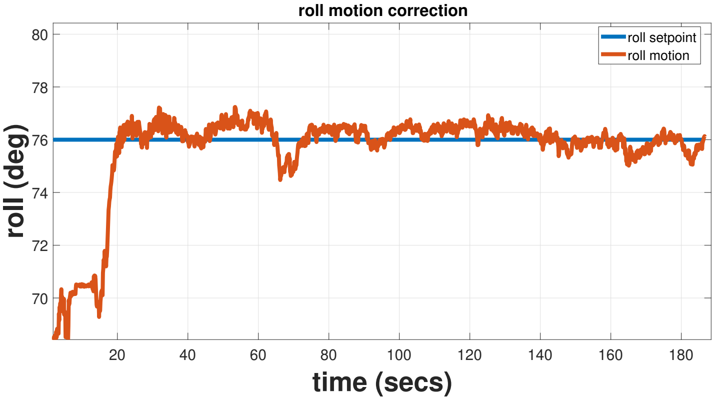


Head roll tracking.

# Conclusions



- Non-invasive soft robot for head motion compensation ✓
- Photons-transparent as opposed to rigid/electro-mechanical devices/robots ✓
- Adaptible under MRI coils for newer MRI-LINACs ✓

# Part III: Robustness Margins and Robust Deep Policies



- Robustness Margins and Robust Deep Policies for Nonlinear Control

# The robustness conundrum



- How to know *a priori* a policy's robustness limits?

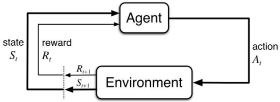


- How to inculcate robustness into multistage decision policies?

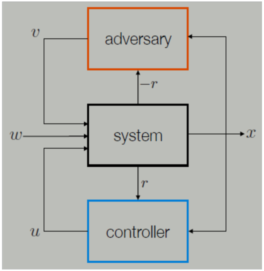

# Problem Setup



- To quantify the brittleness, we optimize the stage cost

$$\max_{\mathbf{v}_t \sim \psi \in \Psi} \left[ \sum_{t=0}^{T} \underbrace{c(\boldsymbol{x}_t, \mathbf{u}_t)}_{\text{nominal}} - \gamma \underbrace{g(\mathbf{v}_t)}_{\text{adversarial}} \right]$$

- To mitigate lack of robustness, we optimize the *cost-to-go*

$$\mathcal{J}_t(\boldsymbol{x}_t, \pi, \psi) = \min_{\mathbf{u}_t \sim \boldsymbol{\pi}} \max_{\mathbf{v}_t \sim \psi} \left( \sum_{t=0}^{T-1} \ell_t(\boldsymbol{x}_t, \mathbf{u}_t, \mathbf{v}_t) + L_T(\boldsymbol{x}_T) \right),$$

- and seek a saddle point equilibrium policy that satisfies

$$\mathcal{J}_t(\boldsymbol{x}_t, \pi^*, \psi) \leq \mathcal{J}_t(\boldsymbol{x}_t, \pi^*, \psi^*) \leq \mathcal{J}_t(\boldsymbol{x}_t, \pi, \psi^*),$$

# Results: Brittleness Quantification

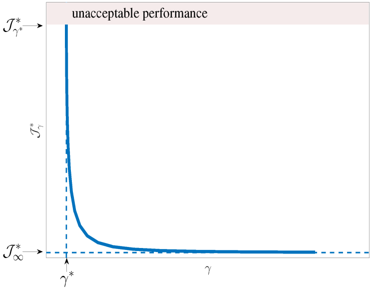


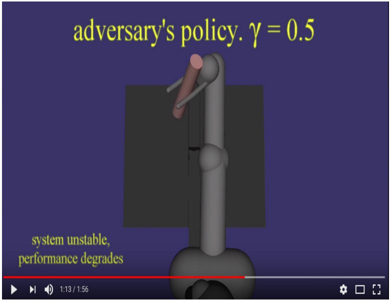

# Results: Iterative Dynamic Game



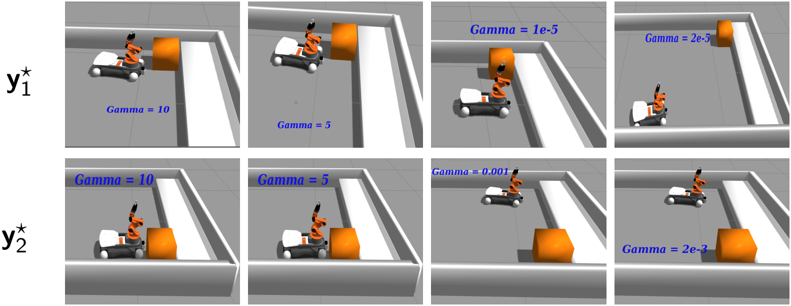


End pose of the KUKA platform with our iDG formulation given different goal states and $\gamma$-values

# Future Work: MRI/RT Immobilization



- Explore multiple parallel robot mechanisms for head motion correction.
- Adopt iterative dynamic game approach [Ogunmolu et al. (2018)] for solving robust controller for head stabilization.
- Build on Freeman and Kokotovic's point-wise min-norm robust control lyapunov function to realize a meaningful value function in deep policies [Freeman and Kokotovic (1996)].

## Conclusions



- Designed a non-invasive soft robot for head motion compensation in IMRT/emerging MRI-LINACs ✓
- Photons-transparent; Adaptible under MRI coils for newer MRI-LINACs ✓
- Fast inference of beam orientations in treatment planning: Approx 60 secs beams prediction time✓
- Adapted H-$\infty$ control methods for quantifying the brittleness of deep policies✓
- Devised a min-max-trained deep saddle policy for mitigating model mismatch, transfer errors, and policy sensitivity e.t.c. ✓

# Publications



- **Ogunmolu, Olalekan**, Xinmin Liu, Nicholas Gans, and Rodney D. Wiersma. "Mechanism and Model of a Soft Robot for Head Stabilization in Cancer Radiation Therapy." In *2020 IEEE International Conference on Robotics and Automation (ICRA)*, pp. 4609-4615. IEEE, 2020.
- **Ogunmolu, Olalekan**, and Rodney D. Wiersma. "Kinematics and Kinects of a Continuum Parallel Soft Robot for MRI-LINAC Motion Correction." Working Paper, In *IEEE Transactions on Robotics*, IEEE 2020.
- **Ogunmolu, Olalekan** and Rodney D. Wiersma. "A Real-Time Patient Head Motion Correction Mechanism for MRI-Linac Systems." In *2020 Virtual Joint AAPM|COMP Meeting*,AAPM 2020.
- **Ogunmolu, Olalekan**, Xinmin Liu, Rodney D. Wiersma. "Auto-Determination of the Dextrous WorkSpace in Robotic Stereotactic Radiosurgery." In *2020 Virtual Joint AAPM|COMP Meeting*, AAPM 2020.
- **Ogunmolu, Olalekan**, Nicholas Gans, and Tyler Summers. "Minimax iterative dynamic game: Application to nonlinear robot control tasks." In 2018 *IEEE/RSJ International Conference on Intelligent Robots and Systems (IROS)*, pp. 6919-6925. IEEE, 2018.
- **Ogunmolu, Olalekan**, Nicholas Gans, and Tyler Summers. "Robust zero-sum deep reinforcement learning." *arXiv preprint arXiv:1710.00491* (2017).
- Summers, Tyler, **Ogunmolu, Olalekan**u, Nicholas Gans. "Robustness Margins and Robust Guided Policy Search for Deep Reinforcement Learning." In *IEEE/RSJ International Conference on Robots and Intelligent Systems,(Abstract Only Track)*, vol. 8. 2017.

# Publications

- **Ogunmolu, Olalekan**, Gans, Nicholas, Jiang, Steve, and Gu, Xuejun. "SU-E-J-12: An Image-Guided Soft Robotic Patient Positioning System for Maskless Head-And-Neck Cancer Radiotherapy: A Proof-Of-Concept Study." *Medical Physics* 42, no. 6Part7 (2015): 3266-3266.
- **Ogunmolu, Olalekan P.**, Xuejun Gu, Steve Jiang, and Nicholas R. Gans. "A real-time, soft robotic patient positioning system for maskless head-and-neck cancer radiotherapy: an initial investigation." In *2015 IEEE International Conference on Automation Science and Engineering (CASE)*, pp. 1539-1545. IEEE, 2015.
- **Ogunmolu, Olalekan P.**, Xuejun Gu, Steve Jiang, and Nicholas R. Gans. "Vision-based control of a soft robot for maskless head and neck cancer radiotherapy," In *2016 IEEE International Conference on Automation Science and Engineering (CASE)*, pp. 180-187.IEEE, 2016.
- **Ogunmolu, Olalekan**, Adwait Kulkarni, Yonas Tadesse, Xuejun Gu, Steve Jiang, and Nicholas Gans. "Soft-neuroadapt: A 3-dof neuro-adaptive patient pose correction system for frameless and maskless cancer radiotherapy." In *2017 IEEE/RSJ International Conference on Intelligent Robots and Systems (IROS)*, pp. 3661-3668. IEEE, 2017.
- Almubarak, Yara, Joshi, Aniket, **Ogunmolu, Olalekan**, Gu, Xuejun, Jiang, Steve, Gans, Nicholas, and Tadesse, Yonas. "Design and development of soft robot for head and neck cancer radiotherapy." In *Electroactive Polymer Actuators and Devices (EAPAD)* XX, vol. 10594, p. 1059418. International Society for Optics and Photonics, 2018.

# Publications



Johannes Heinrich, Marc Lanctot, and David Silver. Fictitious self-play in extensive-form games. In *International Conference on Machine Learning*, pages 805–813, 2015.

Sadeghnejad Barkousaraie, Azar and Ogunmolu, Olalekan and Jiang, Steve and Nguyen, Dan. A Fast Deep Learning Approach for Beam Orientation Selection Using Supervised Learning with Column Generation on IMRT Prostate Cancer Patients. *Medical Physics, American Association of Physicists in Medicine*, 2019.

Radhini Chelvarajah, Brigid Leighton, Linda Martin, Wayne Smith, and Rachael Beldham-Collins. Cranial immobilisation—is there a better way? *Radiographer*, 51(1):29–33, 2004.

Xinmin Liu, Andrew H Belcher, Zachary Grelewicz, and Rodney D Wiersma. Robotic stage for head motion correction in stereotactic radiosurgery. In *2015 American Control Conference (ACC)*, pages 5776–5781. IEEE, 2015.

Andrew Belcher. *Patient Motion Management with 6-DOF Robotics for Frameless and Maskless Stereotactic Radiosurgery*. PhD thesis, The University of Chicago, 2017.

Olalekan Ogunmolu and Rodney Wiersma. A Real-Time Patient Head Motion Correction Mechanism for MRI-Linac Systems. In *Joint AAPM | COMP Meeting, Virtual*, 2020.

James Pikul, Itai Cohen, and Robert Shepherd. Stretchable surfaces with programmable texture, May 2 2019. US Patent App. 16/161,029.

PC Parks. Liapunov Redesign of Model Reference Adaptive Control Systems. *IEEE Transactions on Automatic Control*, 11(3):362–367, 1966.

Olalekan Ogunmolu, Adwait Kulkarni, Yonas Tadesse, Xuejun Gu, Steve Jiang, and Nicholas Gans. Soft-NeuroAdapt: A 3-DOF Neuro-Adaptive Patient Pose Correction System for Frameless and Maskless Cancer Radiotherapy. In *IEEE/RSJ International Conference on Intelligent Robots and Systems (IROS), Vancouver, BC, CA*, pages 3661–3668. IEEE, 2017.

Olalekan Ogunmolu, Nicholas Gans, and Tyler Summers. Minimax Iterative Dynamic Game : Application to Nonlinear Robot Control. *IEEE International Conference on Intelligent Robots and Systems*, 2018.

Randy A Freeman and Petar V Kokotovic. Inverse optimality in robust stabilization. *SIAM journal on control and optimization*, 34(4):1365–1391, 1996.